Particle Therapy for the Treatment of Brain Metastases

13

Jeremy Brownstein, Hooney D. Min, Marc Bussiere, and Helen A. Shih

Abbreviations

ASL	Acute Severe Lymphopenia
CIT	Carbon Ion Therapy
IMPT	Intensity Modulated Proton Therapy
IMRT	Intensity Modulated Radiation Therapy
LET	Linear Energy Transfer
MGH	Massachusetts General Hospital
PBS	Pencil Beam Scanning
PBT	Proton Beam Therapy
PSP	Passively Scattered Protons
RBE	Relative Biological Effectiveness
SOBP	Spread-Out Bragg Peak
SRS	Stereotactic Radiosurgery
VMAT	Volumetric Modulated Arc Therapy

J. Brownstein (✉)
Department of Radiation Oncology, Massachusetts General Hospital, Boston, MA, USA

Department of Radiation Oncology, Comprehensive Cancer Center, The Ohio State University, Columbus, Ohio, USA
e-mail: jeremy.brownstein@osumc.edu

H. D. Min
College of Medicine, Seoul National University, Seoul, South Korea

M. Bussiere
Stereotactic Physics, Department of Radiation Oncology, Massachusetts General Hospital, Boston, MA, USA

H. A. Shih
Proton Therapy Centers, Department of Radiation Oncology, Massachusetts General Hospital, Boston, MA, USA

Case Vignettes

Case 1

A fifty-five-year-old gentleman and nonsmoker with metastatic non-small-cell lung cancer initially presented 3 years ago with a persistent cough of 3 months even after asthma medication adjustments and steroids. Workup revealed a right upper lobe lung mass with mediastinal adenopathy, biopsy confirming moderately differentiated adenocarcinoma. Staging revealed several sites of osseous and multiple brain metastases. He received whole-brain radiation therapy 30 Gy in 10 fractions and had no further CNS disease for 3 years while on systemic therapy. On routine staging, he was then found to have developed two new asymptomatic left frontal metastases. He was treated with proton SRS, 18 Gy (RBE) to each lesion, well tolerated and with high conformality, minimizing unaffected brain reirradiation (Fig. 13.1a, b).

Case 2

A forty-six-year-old female presented with BRAF mutant metastatic melanoma, who was initially diagnosed 4 years prior with a pruritic pigmented scalp lesion that was resected. She underwent wide local excision, which was found to be of 5 mm depth and with 2/5 sentinel lymph nodes positive.

Y. Yamada et al. (eds.), *Radiotherapy in Managing Brain Metastases*,
https://doi.org/10.1007/978-3-030-43740-4_13

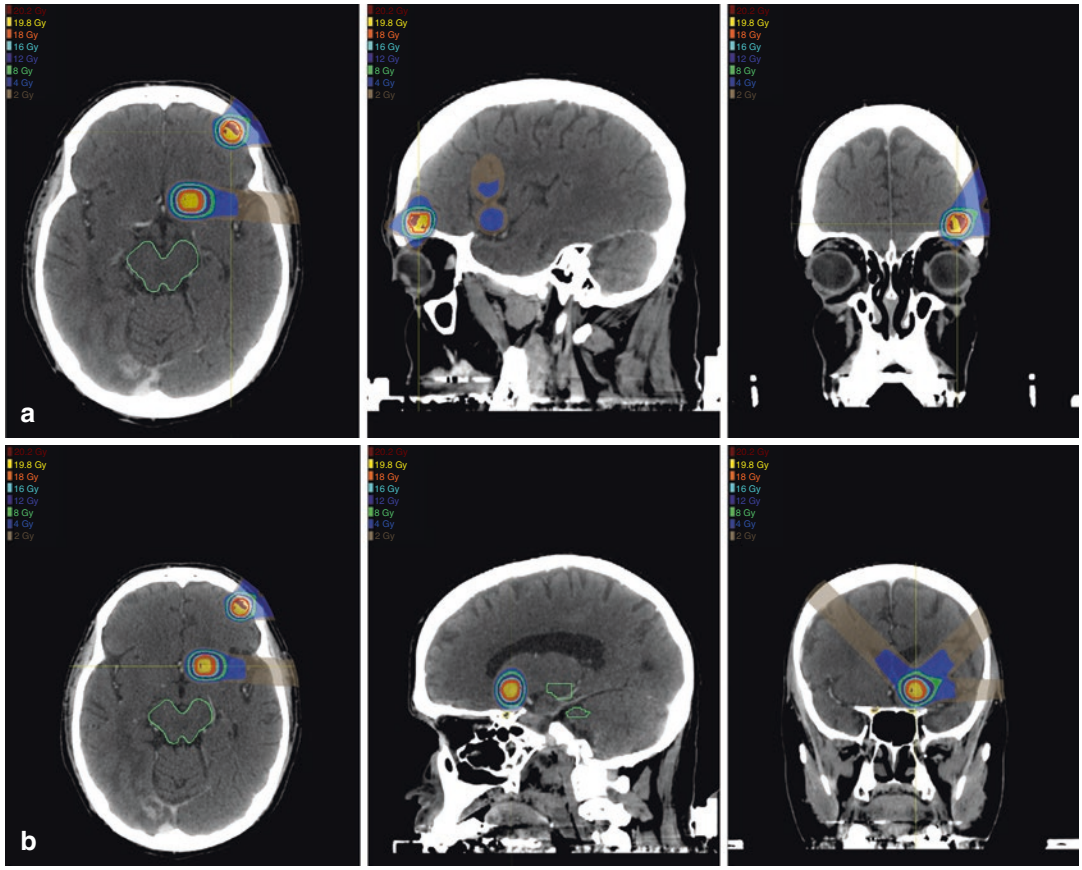

Fig. 13.1 Proton SRS plans of two left frontal non-small-cell lung cancer brain metastases along the anterior skull base treated on the same day: (**a**) lesion just superior to the left orbit and (**b**) lesion just superior to the left optic nerve and anterior to the chiasm. Maximum sparing to the surrounding normal tissues is achieved with proton therapy

Despite more comprehensive local and nodal excision that was negative for additional disease, she recurred with pulmonary metastases 14 months from initial diagnosis, underwent BRAF-directed therapy for 5 months followed by immunotherapy at the time of progression. Four months later, she developed her first intracranial metastases in the right occipital lobe and left thalamus. These were irradiated without incident. One year later, she developed further asymptomatic intracranial disease of a right temporal and left anterior frontal brain metastases. Given the peripheral locations and moderate size of the left frontal lesion, she was treated with proton SRS to minimize collateral brain radiation exposure (Fig. 13.2a, b).

Proton Basics

Dose Distribution

In Proton Beam Therapy (PBT), a beam of protons is accelerated to high energies using either a *cyclotron* or a *synchrotron,* and is then modulated, focused and shaped to target the desired treatment volume. Protons in PBT interact with matter primarily via *proton–electron reactions* and thus deposit dose differently than do photons used in external beam radiation therapy (i.e., megavoltage X-rays and high energy Gamma Rays), which primarily interact via *Compton scattering* [1]. Photons are deeply penetrating.

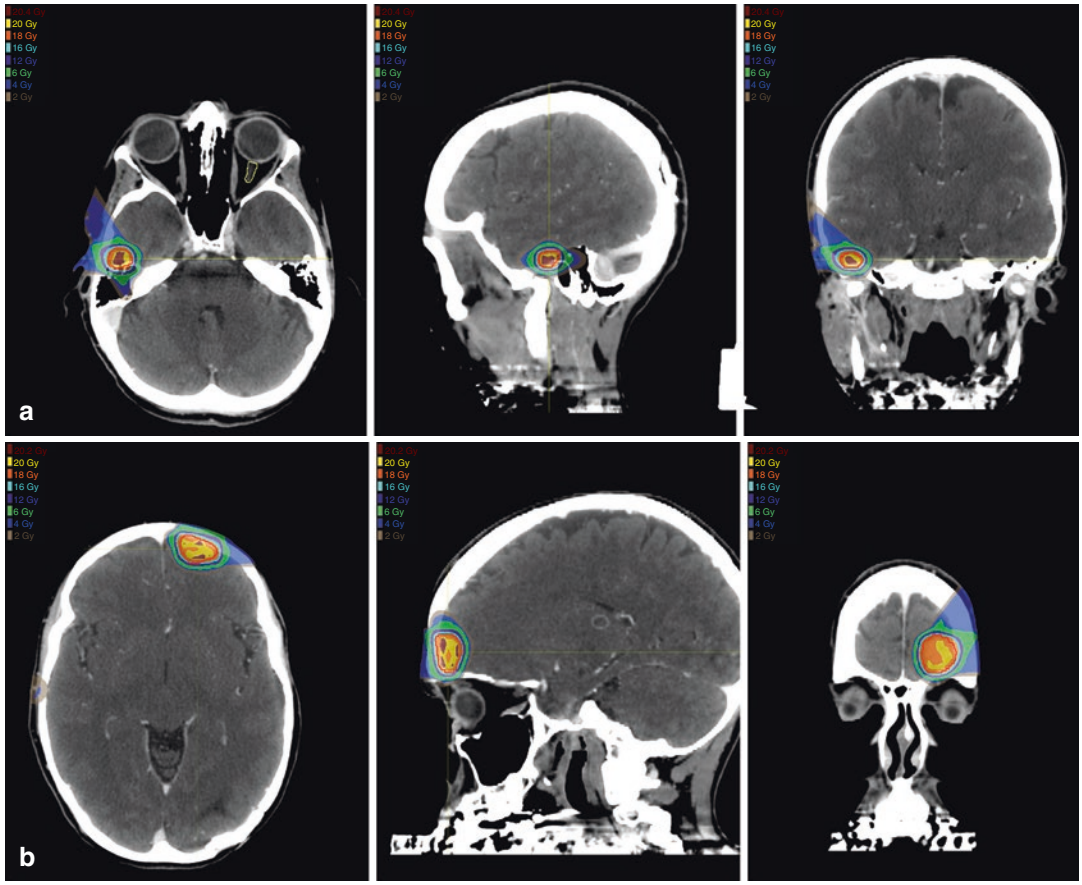

Fig. 13.2 Proton SRS plans of two melanoma brain metastases treated on the same day: (**a**) a lesion of the right temporal skull base and anterior to the cochlea and (**b**) an intermediate size lesion along the left anterior frontal convexity. Each plan achieves maximal sparing of the surrounding brain

Following an initial buildup, the dose they deposit gradually decreases throughout the full length of the beam path [2]. On the other hand, protons slow down as they traverse tissues and eventually halt. Contrary to the gentle slope of photon dose distributions, the dose deposited by protons increases dramatically as the proton beam slows, peaking in a narrow burst (known as the Bragg peak) before plummeting to zero as the protons abruptly stop (Fig. 13.3). Since the range of protons in tissues is finite with minimal dose deposited beyond the Bragg peak, protons can be used to treat a target while sparing normal tissues just beyond the target, yielding a potential advantage as compared to photons.

Scattering and Modulation

The water-equivalent depth of the Bragg peak is energy-dependent and roughly proportional to the initial energy squared [D_{WET} [3] = 0.0022 × E (MeV)$^{1.77}$] [4]. Monoenergetic protons exit the accelerator in the form of a "pencil beam," which is only a few millimeters in diameter. Unaltered, this beam would create a very narrow field with a Bragg peak depositing dose in tissue spanning only a few millimeters in depth. As most clinically relevant targets span 1–20 cm in the traverse and longitudinal axes, a monoenergetic pencil beam will not suffice for most treatments. Therefore, a polyenergetic beam must be

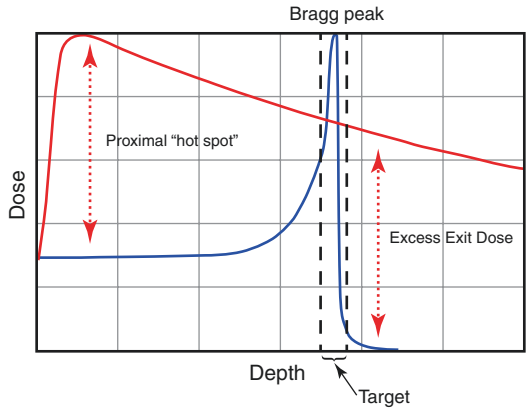

Fig. 13.3 Dose distribution of therapeutic photon and proton beams. Dose as a function of depth is demonstrated for photons (red) and protons (blue). For photons, the maximum dose occurs proximal to the target. Within the beam path, this "hot spot" will receive a higher dose than the target. Photons also continue to deposit dose distal to the target, resulting in unnecessary exit dose. Within a proton beam, dose increases with increasing depth, reaching a maximum in the Bragg peak. The choice of beam energy is chosen such that the Bragg peak falls within the target. Distal to the Bragg peak, dose decreases precipitously, resulting in minimal exit dose

employed with energies chosen to create overlapping Bragg peaks throughout the depth of the target, and the beam must be altered to cover the width of the treatment volume. This can be achieved using scattering and scanning technology.

Scattering, also referred to as *passive scattering*, was the mainstream therapeutic technology for the first several decades of clinical application. A homogeneous dose distribution in depth can be created by superimposing monoenergetic beams of differing energies. This can be achieved by introducing one of a number of modulation devices. One common method passes the pencil beam through a *spinning compensator wheel* that contains spokes of varying thickness. As the pencil beam encounters progressively thicker spokes, the resultant protons will have incrementally lower energy and will produce ever-shallower Bragg peaks. The arc-length of each spoke reflects the relative weight of the corresponding peak. Alternatively, a pencil beam can be passed through a *ridge filter* – a static block with an echinate surface of repeating finely spaced ridged spikes. Protons that have encountered the tip of a spike will have lower energy than protons encountering a valley. In both methods, a number of Bragg peaks are produced which combine to form a so-called "spread-out Bragg peak" (SOBP). Modulators devices are specifically designed such that the SOBP produces a uniform physical dose throughout the breadth of the target volume (Fig. 13.4). For a detailed description of passive scatter techniques, please refer to Refs. [5–7]. With passive scattering, the narrow polyenergetic beam is broadened by passing through one or more scattering devices which helps spread the dose profile laterally (i.e., *double scattering*). Patient and field-specific *apertures* made of brass, Cerrobend, or created with a multileaf collimator conform the beam to the lateral contours of the target and around critical structures. Patient- and field-specific *range compensators* fabricated from plastics or wax are also used to further conform the SOBP to the distal edge of the target [7].

In contrast, *scanning* systems (i.e., Pencil Beam Scanning or PBS) utilize bending magnets to sweep the monoenergetic pencil beam laterally across the treatment field (much like the electron beam is swept across a phosphorescent screen in an old-fashioned cathode-ray television), allowing the dose to be "painted" onto tissue at a given depth. The deep surface of the target is treated first with the highest energy protons. The primary beam energy is then decreased incrementally and successive shallower layers are similarly painted with the dose. As one can modulate the intensity of the pencil beam as it sweeps across the field and/or modulates the time the beam spends at each location, this technique is often referred to as *intensity modulated proton therapy* (IMPT). Like X-ray-based intensity modulated radiation therapy (IMRT), IMPT also employs inverse planning and optimization; however, due to the ability of protons to form Bragg peaks, IMPT can utilize fewer fields and inherently eliminates exit dose, significantly decreasing integral dose as compared to IMRT [8]. While there are advantages and disadvantages to both passive scattering and scanning systems, most newer systems employ scanning technology (i.e., IMPT), as this

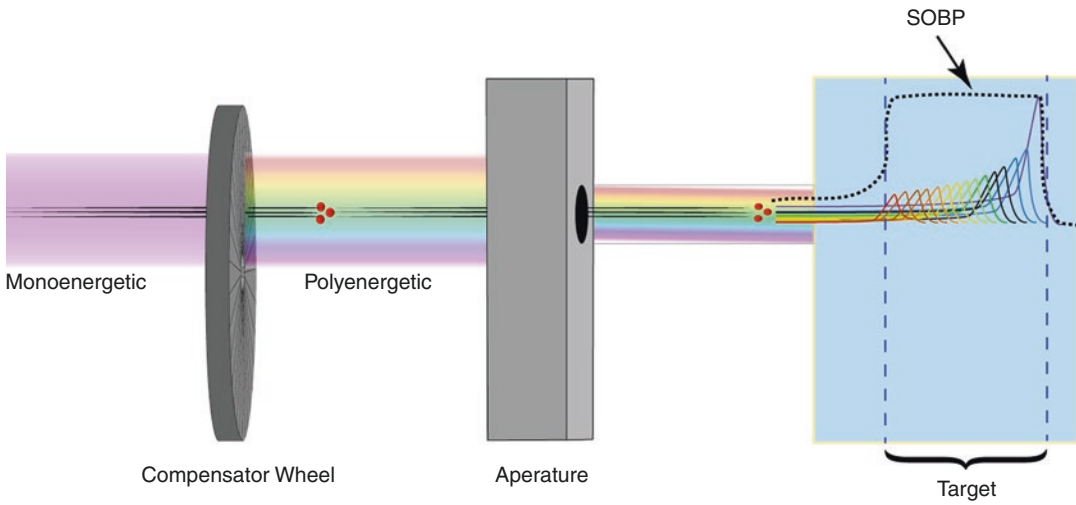

Fig. 13.4 Schematic of a passively modulated proton beam. A monoenergetic proton beam leaving a cyclotron or synchrotron interacts with a spinning modulation wheel (variable depth of modulator wheel not depicted). The resultant polyenergetic beam is collimated through an aperture before encountering the target. The configuration of the modulation wheel is specifically chosen to yield of a spectrum of energies that deposit Bragg peaks throughout the breadth of the target, called a "spread-out Bragg peak" (SOBP). (Image modified with permission from the following Brownstein et al. [12])

technique allows for far greater conformation of both the distal AND the proximal edge of target. Because most passively scattered beams have *uniform range modulation* (i.e., the "thickness" of the SOBP is approximately constant), using a range compensator to conform the distal SOBP to the deep contour of a target will, by necessity, impact proximal SOBP as well – potentially resulting in hot spots superficial to the target. Conversely, a scanning platform affords more freedom in the placement of pencil beam segments, allowing for *variable range modulation*. Furthermore, IMPT enables variable dose intensity to be delivered to a target within a given treatment (i.e., simultaneous integrated boost) [9], and allows for additional optimization to account for range uncertainties [10] and/or incorporate biological factors [11] (discussed below).

Biological Factors

There are many forms of ionizing radiation, ranging from massless photons to heavy atomic nuclei traveling at relativistic speeds. The biological impacts of radiation depend not only on the quantity of dose delivered but also on how it interacts with matter. Photons deposit energy sparsely, imparting DNA damage that can frequently be repaired (i.e., single strand breaks). Heavy ions are more potent than photons because, within their Bragg peak, they deposit radiation in dense ionization tracks that can impart highly clustered, irreparable DNA damage (i.e., double strand breaks, dicentric rings, etc.). For example, the damage imparted by carbon and heavier ions can be equivalent to the damage caused by a threefold higher dose of X-rays [12]. Heavy ions are thus termed as high Linear Energy Transfer (LET) radiation in that a large amount of energy is deposited over a shorter distance compared to low LET radiation photons [13]. To compare doses between modalities, the Relative Biological Effectiveness (RBE) is defined as the dose ratio of X-rays to the particle of interest required to cause the same biological effect (i.e., in the above example, the RBE of carbon ions is 3 because a threefold higher dose of X-rays is required to induce the same damage) [14].

Protons are considered "low LET" radiation but are nonetheless more potent than X-rays. In most clinical applications, protons are generally

assumed to have a constant RBE of 1.1, implying that a given proton treatment is biologically equivalent to a 10% higher dose of X-rays [15]. For this reason, proton doses are frequently referenced in Gy (RBE) to specify the X-ray equivalent dose [14]. However, a growing body of literature suggests that assuming a uniform RBE of 1.1 may ignore clinically relevant nuances. Similar to the carbon ions, as a proton slows along its path it deposits energy with increasing intensity and density. Thus, slow-moving protons approaching their end-of-range have a higher LET and their RBE can be greater than 1.1. Since the distal edge of a target volume has a greater fraction of slow-moving protons than the proximal edge, the RBE tends to increase with increasing depth assuming the target volume has uniform physical dose. Paganetti et al. (2014) described the increase in proton RBE over the course of a uniform SOBP: the RBE is ~1.1 in the entrance region, ~1.15 in the center, ~1.35 in the distal edge, and ~1.7 in the distal fall off [16]. Thus, placing the distal edge of a target volume in a radiosensitive organ under the assumption of a uniform RBE of 1.1 may result in a biologically effective overdose of 20%. Peeler et al. (2016) reviewed a series of pediatric patients treated with PBT for ependymoma and retrospectively calculated LET using Monte Carlo simulations. They noted a significant association on univariate analysis between treatment-related changes on T2 MRI and higher LET_{max} within their CTV [17].

RBE is complex and is dependent on many variables. In addition to LET and dose-per-fraction, RBE is also influenced by biological factors such as histology, the tissue's intrinsic radiosensitivity/capacity for repair, and tumor oxygenation [18]. Recently, several groups have noted that cytogenetics may also impact RBE. Mutations in the DNA Homologous Repair and Fanconi Anemia pathways result in increased susceptibility to proton-mediated cell kill and thus a higher RBE [3, 19]. While many RBE modeling techniques are currently under investigation that include both physical and biological factors, there remains no clear consensus as to how to incorporate a variable RBE into proton treatment planning and most centers continue to assume a uniform RBE of 1.1 [20].

Proton Stereotactic Radiosurgery Techniques

Immobilization and Image Guidance

Effective immobilization is of critical importance to ensure accurate target localization. Compared with photon SRS, errors in setup can have an even greater impact on the dose distribution as the depth of the Bragg peak is extremely sensitive to changes in depth and density of tissues proximal to the target. The immobilization devices used for proton SRS are specially designed to limit particle scattering. An example of an immobilization frame that has been developed for proton therapy of brain tumors is the Massachusetts General Hospital (MGH) modified Gill-Thomas-Cosman frame, comprising a rounded carbon fiber occipital support, low-density cushion, and a dental mold fixed to a stereotactic cranial ring (Fig 13.5a). This device is used in the treatment of intracranial targets that do not extend to the base of the skull but requires that the patient has good dentition to create excellent and reproducible immobilization. Alternative fixation devices, which do not use dental fixation, make use of thermoplastic masks and custom occipital cushions for a comfortable yet reproducible immobilization while being designed with consideration for the sensitivities associated with proton therapy [21].

Cone Beam CT and automated localization systems are now being integrated into many newer proton therapy platforms [22]. However, these developments are recent and some established proton centers continue to employ calvarial fiducial markers to rigorously triangulate patient position and ensure accurate treatment delivery (Fig 13.5b). Fiducial marker placement can be performed as an outpatient procedure by a neurosurgeon in 15–20 minutes with minimal risk of complications.

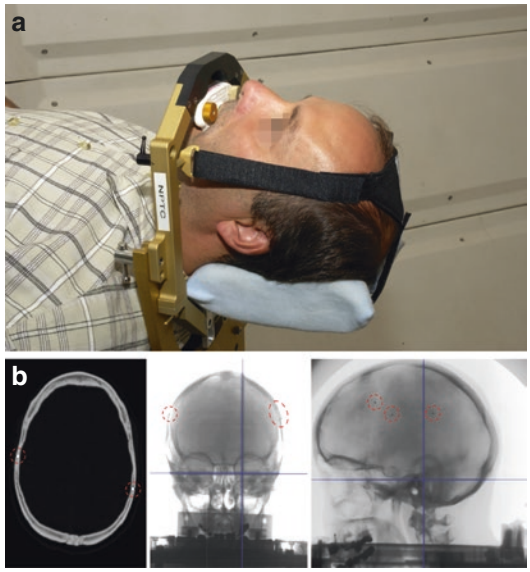

Fig. 13.5 Proton treatment immobilization and localization. (**a**) The modified Gill-Thomas-Cosman mask achieves reproducible noninvasive immobilization with a Velcro strap that secures the patient's forehead and a custom dental tray that rigidly associates with his/her dentition. (**b**) Fiducials are placed via a minimally invasive procedure deep to the outer table of the calvarium. CT (left panel) demonstrates well-placed fiducials (red circles). Pretreatment onboard kV imaging (middle and right panel) sets the isocenter by aligning to fiducials (red circles) with ± 0.5 mm accuracy

Dosimetric Considerations

As intracranial tumors often reside in close proximity to important avoidance structures, the best-achievable radiation plans may necessitate either incomplete target coverage or exceeding normal tissue constraints. To this end, many groups have evaluated which modality – photons or protons – can best maximize intracranial target coverage while minimizing normal tissue toxicities. Bolsi et al. simultaneously planned 12 cases (5 meningiomas, 5 acoustic neuromas, and 2 pituitary adenomas) with 3D conformal photon radiotherapy, IMRT, stereotactic arc photon therapy, spot-scanning protons, and passively scattered protons. All modalities had excellent target coverage but those planned with protons demonstrated significantly lower mean radiation dose to the brainstem, eyes, and uninvolved brain [23]. Freund et al. compared 13 cases of pediatric CNS tumors planned for fractionated radiotherapy with contemporary Volumetric Modulated Arc Therapy (VMAT), passively scattered protons (PSP), and IMPT. Compared to VMAT, both PSP and IMPT had significantly higher maximum brain dose, lower brain volume receiving low dose radiation, and a lower predicted risk of brain necrosis [24].

Proton Beam Dosimetry

While PBS systems are adept at treating irregular volumes, brain metastases are frequently small and spherical, and can thus be approached with simpler modulation techniques. S*ingle scattering* systems are well suited for irradiating small targets that do not require the lateral beam spreading needed for larger lesions. Here a pencil beam is passed through low-Z material to achieve the desired Bragg peak pull-back. While the resultant field has a nonuniform dose distribution, the central portion is sufficiently flat and can be collimated to treat small targets with excellent dose homogeneity. Compared to more complicated scanning techniques, single scattering systems can be designed with smaller effective source diameters and larger source-to isocenter distances to produce a narrower lateral penumbra at shallow depth compared to double scattering systems. Safai et al. also noted that for targets <14 cm depth in water (i.e., most intracranial targets), the lateral penumbra of a collimated passively scattered beam is sharper compared to that of a pencil beam, even for a smaller PBS beam spot of 3 mm. For example, they found that for a target at 4 cm depth in water, the lateral 80% – 20% penumbra of PBS (3 mm spot size) was 1 cm compared to ~3 mm for a collimated beam [25]. Others have found that adding a collimator to a PBS platform significantly improves lateral penumbra at depths <11 cm in water [26]. The authors note that these observations cannot be broadly applied, as proton beam profiles are highly dependent on the specifics of the individual system.

Clinical Applications

Benign Intracranial Lesions

Owing to their favorable dose distribution, proton therapy platforms are of interest in stereotactic radiosurgery. Protons are a particularly appealing option for the treatment of benign intracranial lesions as patients often have an excellent prognosis and limiting dose to uninvolved brain becomes a greater priority. MGH has published several series detailing their experience with proton-SRS in the treatment of vestibular schwannomas [27], pituitary adenomas [28, 29], and arteriovenous malformations [30, 31]. For a detailed and comprehensive clinical discussion regarding the proton-SRS, please refer to the following [32].

Proton SRS for Brain Metastases

There are limited data regarding the use of proton stereotactic radiosurgery for the treatment of brain metastases. MGH has published the only series to date, reporting their experience treating 815 brain metastases in 370 patients between 1991 and 2016 [33]. Median age of patients included was 61 and most had an excellent performance status with 2/3 having Karnofsky Performance Status $\geq$ 80%. A variety of tumor histologies were represented with a non-small-cell lung cancer implicated in a plurality of patients (34%) followed by melanoma (28%) and breast cancer (17%). Approximately half of patients had no extracranial disease and approximately one half only had a single metastasis.

Patients were treated at the Harvard Cyclotron Laboratory until construction of Francis H. Burr Proton Center at MGH main campus was completed in 2001. Patients included in this series were immobilized with different techniques depending upon the clinical context (described above). All patients underwent placement of calvarial fiducial markers to ensure accurate setup with orthogonal X-rays. Target volumes ranged 0.02–23.3 cm^3 (mean 1.6 cm^3; median 0.6 cm^3) and delivered dose ranged 8–28 Gy (mean 17.3; median 18 Gy (RBE)).

With a median follow up of 9.2 months, oncologic outcomes were comparable to those reported in photon SRS series. Local failure at 6 and 12 months was 4.3% and 8.5%, respectively; distant CNS failure rates at 6 and 12 months was 39% and 48%, respectively; and median overall survival was 12.4 months. Treatments were well tolerated with only 11% incidence of Grade 2+ acute toxicity, and pathologically confirmed radionecrosis occurring in 3.6% at 1 year. The authors conducted retrospective analysis of 10 patients with 3–4 brain metastases, comparing the achieved proton dose distribution with the distribution achievable using photon-SRS techniques. They noted a significantly lower volume of brain receiving 4 Gy with protons compared to photons. Figure 13.6 demonstrates a similar comparison of one such patient who was initially treated with proton SRS and was subsequently re-planned post hoc with contemporary high-density MLC VMAT.

Heavy Charged Particle SRS for Brain Metastases

There is growing interest in the use of heavier charged particles to treat certain tumors due to their improved dosimetric and radiobiological properties. There are 11 treatment centers in Europe and Asia that utilize Heavy Ion Therapy such as carbon ions, with several more currently under construction [34]. Compared to protons, carbon ions have sharper lateral penumbrae, and have a significantly higher RBE within their Bragg peaks. These advantages make carbon ion therapy (CIT) suitable for treating radio-resistant tumors adjacent critical structures [35]. A retrospective study of patients with low/intermediate grade skull base chondrosarcoma treated with CIT at Heidelberg Ion Beam Therapy Center demonstrated local control rates of 96% and 90% at 3 and 4 years, respectively [36], comparing favorably to patients treated with protons [37, 38]. However, to our knowledge, there are no large published series of patients with brain metastases treated with CIT or other heavy ions. While doing so would be technically feasible, it may not be practical, as availability of CIT is scarce, and this

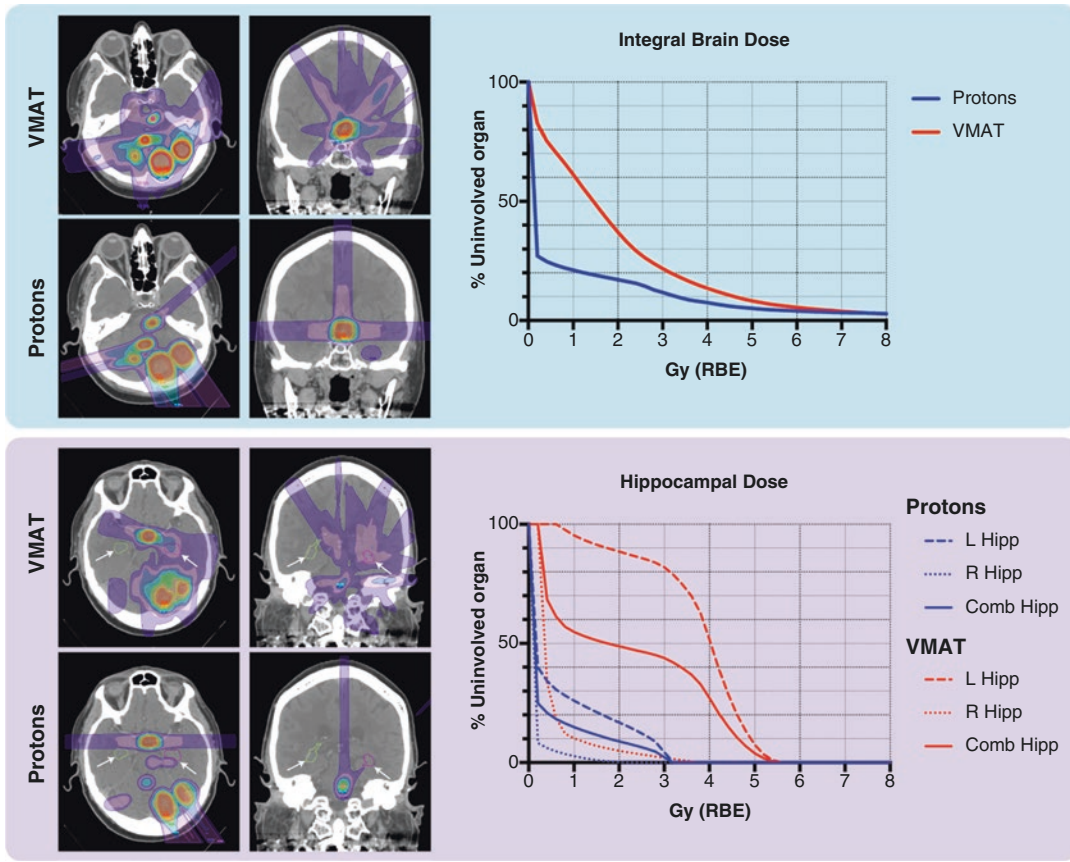

Fig. 13.6 Comparison of Proton-SRS vs. VMAT-SRS in a patient with multiple brain metastases. Blue box: Representative slices showing the dose distribution of VMAT plan (upper panels) and protons (lower panels). DVH (right) demonstrates that the proton plan yields a lower volume of uninvolved brain receiving low doses compared with photons (mean dose 0.96 vs 2.03 Gy). Purple panel: Representative slices showing the dose distribution of VMAT plan (upper panels) and protons (lower panels) with the hippocampi labeled with white arrows. DVH (right) demonstrates that the proton plan yields a lower dose to left hippocampus (mean dose 0.68 vs. 3.75 Gy, respectively), right hippocampus (mean dose 0.07 vs. 0.54 Gy, respectively), and bilateral hippocampi (mean dose 0.39 vs. 2.22 Gy, respectively). Of note, neither proton nor VMAT plans were specifically optimized to avoid the hippocampi

modality is unlikely to offer a significant advantage over other radiosurgery platforms.

Discussion

Some physicians have raised concerns vis-a-vis routinely employing proton-SRS in the treatment of brain metastases. In response to the Harvard experience presented above, Kirkpatrick et al. reiterate that local control and intracranial progression with protons are not improved compared to historical series treating brain metastases with photon-SRS – an expected finding given that proton patients were treated with similar, if not more modest doses [39]. They further point out that data are lacking as to whether the decreased integral dose seen with protons translates into improved neurocognition, especially given the poor prognosis associated with brain metastases. They hypothesize that the cost for proton centers to deliver proton-SRS may be much higher than photon-SRS while yielding similar outcomes.

The authors of this chapter agree that there are currently insufficient data to justify routinely recommending proton-SRS over photon-SRS in the

treatment of brain metastases. In most instances, advanced photon platforms employing VMAT can easily and efficiently simultaneously target multiple metastases with highly conformal radiotherapy utilizing only a single or multiple isocenter(s). Since many such platforms frequently include on-board image guidance with cone-beam CT and surface tracking, invasive immobilization and/or fiducial markers are unnecessary.

Despite improvements in photon delivery and image-guided therapy, there are specific instances where protons may be indicated in the treatment of brain metastases. PBT can offer a dosimetric advantage, particularly with large or irregular targets [40] and can facilitate sparing of critical structures within a modest proximity of the treatment volume [41]. Thus, proton-SRS may facilitate ablative treatment of brain metastases for certain patients with a disadvantageous tumor distribution in whom photon-SRS cannot be safely delivered.

Advances in systemic therapy have led to longer survival times for many patients with brain metastases. Sperduto et al. have recently updated the Disease Specific – Grade Prognostic Assessment (DS-GPA) for non-small-cell lung cancer. Those in the highest prognostic group from *Alk*-mutated or *EGFR*-mutated adenocarcinoma (DS-GPA 3.5–4) have a median survival of 47 months, including some afflicted with >4 brain metastases [42]. Similarly, those in the favorable prognostic group with metastatic Her2+ cancer have a median survival of 27 months [43]. With new successes in targeted systemic therapies, there is an ever-growing population of patients with "favorable risk" metastatic disease who may live with their cancer for many years, even after developing brain metastases. For such patients, it will be important to explore whether employing proton-SRS to decrease integral brain dose will lead to tangible improvements in neurocognitive outcomes.

Excess integral dose can have deleterious effects that extend beyond uninvolved brain. Under physiological conditions, the brain receives approximately 16% of cardiac output with a heart–heart transit time of approximately 30 seconds [44]. Yovino et al. sought to quantify the unintentional radiation dose imparted to circulating lymphocytes during a course of radiotherapy for malignant glioma. Through careful modeling, they calculated that the mean dose of radiation to circulating lymphocytes was ~2 Gy, which would be expected to kill half of the exposed lymphocytes; and 99% of lymphocytes received >0.5 Gy, which would be expected to kill at least 10% of exposed lymphocytes [45]. Huang et al. observed and employed a logistic regression of 183 patients with high-grade glioma and demonstrated a significant association between V25 Gy and development of acute severe lymphopenia (ASL) [46, 47]. This study and others [48] have also described a correlation between ASL and worse overall survival. Of note, the integral radiation doses of uninvolved brain in patients receiving fractionated treatment for glioma are far higher than those anticipated with photon SRS for brain metastases. Nonetheless, with the growing role immunotherapy in metastatic patients, it is increasingly important to be cognoscente of how radiotherapy impacts the immune system.

In conclusion, proton SRS is an effective and safe treatment for brain metastases. While there are currently no indications for its routine use over photon SRS, protons may better facilitate safe treatment of large volume disease and may yield a lower integral dose for patients with several small volume metastases. Further investigation is needed to determine if this lower integral dose translates into superior neurocognitive outcomes or better protects anti-cancer immunity.

Key Points

- PBT has a dosimetric advantage compared to photon radiotherapy. Unlike deeply penetrating photons that deposit dose throughout the entirety of their beam path, protons halt at a specific depth depositing most of their dose at the end of range within a narrow Bragg peak. This results in minimal exit dose deposited distal to the target.

- Proton-SRS is a safe and effective treatment for brain metastases, resulting in better low-dose sparing and similar oncologic outcomes compared to photon-SRS.
- Given that advanced photon-SRS platforms are widely available and can deliver highly conformal treatments that frequently meet all desired constraints, the authors of this chapter do not recommend routinely employing proton-SRS in the treatment of brain metastases.
- Off protocol Proton-SRS should only be considered in cases where ablative treatment is indicated, but photon-SRS cannot achieve desired constraints.
- Future studies are needed to determine if the decreased exit dose afforded by proton-SRS can better protect antitumor immunity or can better spare long-term neurocognition in patients with a favorable prognosis.

References

1. Newhauser WD, Zhang R. The physics of proton therapy. Phys Med Biol. 2015;60(8):R155–209.
2. Almond PR, Biggs PJ, Coursey BM, Hanson WF, Huq MS, Nath R, et al. AAPM's TG-51 protocol for clinical reference dosimetry of high-energy photon and electron beams. Med Phys. 1999;26(9):1847–70.
3. Willers H, Allen A, Grosshans D, McMahon SJ, von Neubeck C, Wiese C, et al. Toward A variable RBE for proton beam therapy. Radiother Oncol. 2018;128(1):68–75.
4. Bortfeld T. An analytical approximation of the Bragg curve for therapeutic proton beams. Med Phys. 1997;24(12):2024–33.
5. Wilson RR. Radiological use of fast protons. Radiology. 1946;47(5):487–91.
6. Larsson B. Pre-therapeutic physical experiments with high energy protons. Br J Radiol. 1961;34:143–51.
7. Paganetti H. Proton therapy physics. Boca Raton: CRC Press; 2016.
8. Trofimov A, Bortfeld T. Optimization of beam parameters and treatment planning for intensity modulated proton therapy. Technol Cancer Res Treat. 2003;2(5):437–44.
9. Madani I, Lomax AJ, Albertini F, Trnkova P, Weber DC. Dose-painting intensity-modulated proton therapy for intermediate- and high-risk meningioma. Radiat Oncol. 2015;10:72.
10. Paganetti H. Range uncertainties in proton therapy and the role of Monte Carlo simulations. Phys Med Biol. 2012;57(11):R99–117.
11. Giantsoudi D, Grassberger C, Craft D, Niemierko A, Trofimov A, Paganetti H. Linear energy transfer-guided optimization in intensity modulated proton therapy: feasibility study and clinical potential. Int J Radiat Oncol Biol Phys. 2013;87(1):216–22.
12. Brownstein JM, Wisdom AJ, Castle KD, Mowery YM, Guida P, Lee CL, et al. Characterizing the potency and impact of carbon ion therapy in a primary mouse model of soft tissue sarcoma. Mol Cancer Ther. 2018;17(4):858–68.
13. Durante M, Loeffler JS. Charged particles in radiation oncology. Nat Rev Clin Oncol. 2009;7(1):37–43.
14. International Atomic Energy Agency. Dose reporting in ion beam therapy. Vienna: International Atomic Energy Agency; 2007.
15. Paganetti H, Niemierko A, Ancukiewicz M, Gerweck LE, Goitein M, Loeffler JS, et al. Relative biological effectiveness (RBE) values for proton beam therapy. Int J Radiat Oncol Biol Phys. 2002;53(2):407–21.
16. Paganetti H. Relative biological effectiveness (RBE) values for proton beam therapy. Variations as a function of biological endpoint, dose, and linear energy transfer. Phys Med Biol. 2014;59(22):R419–72.
17. Peeler CR, Mirkovic D, Titt U, Blanchard P, Gunther JR, Mahajan A, et al. Clinical evidence of variable proton biological effectiveness in pediatric patients treated for ependymoma. Radiother Oncol. 2016;121(3):395–401.
18. Hall EJ, Giaccia AJ. Radiobiology for the radiologist. Philadelphia: Wolters Kluwer Health/Lippincott Williams & Wilkins; 2012.
19. Fontana AO, Augsburger MA, Grosse N, Guckenberger M, Lomax AJ, Sartori AA, et al. Differential DNA repair pathway choice in cancer cells after proton- and photon-irradiation. Radiother Oncol. 2015;116(3):374–80.
20. McMahon SJ, Paganetti H, Prise KM. LET-weighted doses effectively reduce biological variability in proton radiotherapy planning. Phys Med Biol. 2018;63(22):225009.
21. Yerramilli D, Bussière MR, Loeffler JS, Shih HA. Proton beam therapy (for CNS tumors). In: Chang EL, Brown PD, Lo SS, Sahgal A, Suh JH, editors. Adult CNS radiation oncology: principles and practice. Cham: Springer International Publishing; 2018. p. 709–22.
22. Hua C, Yao W, Kidani T, Tomida K, Ozawa S, Nishimura T, et al. A robotic C-arm cone beam CT system for image-guided proton therapy: design and performance. Br J Radiol. 2017;90(1079):20170266.
23. Bolsi A, Fogliata A, Cozzi L. Radiotherapy of small intracranial tumours with different advanced techniques using photon and proton beams: a treatment planning study. Radiother Oncol. 2003;68(1):1–14.

24. Freund D, Zhang R, Sanders M, Newhauser W. Predictive risk of radiation induced cerebral necrosis in pediatric brain cancer patients after VMAT versus proton therapy. Cancers. 2015;7(2):617–30.
25. Safai S, Bortfeld T, Engelsman M. Comparison between the lateral penumbra of a collimated double-scattered beam and uncollimated scanning beam in proton radiotherapy. Phys Med Biol. 2008;53(6):1729–50.
26. Winterhalter C, Lomax A, Oxley D, Weber DC, Safai S. A study of lateral fall-off (penumbra) optimisation for pencil beam scanning (PBS) proton therapy. Phys Med Biol. 2018;63(2):025022.
27. Weber DC, Chan AW, Bussiere MR, Harsh IVGR, Ancukiewicz M, Barker IIFG, et al. Proton beam radiosurgery for vestibular schwannoma: tumor control and cranial nerve toxicity. Neurosurgery. 2003;53(3):577–88.
28. Wattson DA, Tanguturi SK, Spiegel DY, Niemierko A, Biller BMK, Nachtigall LB, et al. Outcomes of proton therapy for patients with functional pituitary adenomas. Int J Radiat Oncol Biol Phys. 2014;90(3):532–9.
29. Petit JH, Biller BM, Yock TI, Swearingen B, Coen JJ, Chapman P, et al. Proton stereotactic radiotherapy for persistent adrenocorticotropin-producing adenomas. J Clin Endocrinol Metab. 2008;93(2):393–9.
30. Hattangadi-Gluth JA, Chapman PH, Kim D, Niemierko A, Bussière MR, Stringham A, et al. Single-fraction proton beam stereotactic radiosurgery for cerebral arteriovenous malformations. Int J Radiat Oncol Biol Phys. 2014;89(2):338–46.
31. Hattangadi JA, Chapman PH, Bussière MR, Niemierko A, Ogilvy CS, Rowell A, et al. Planned two-fraction proton beam stereotactic radiosurgery for high-risk inoperable cerebral arteriovenous malformations. Int J Radiat Oncol Biol Phys. 2012;83(2):533–41.
32. Shih HA, Chapman PH, Loeffler JS. Proton beam radiosurgery: clinical experience. In: Lozano AM, Gildenberg PL, Tasker RR, editors. Textbook of stereotactic and functional neurosurgery. Berlin, Heidelberg: Springer Berlin Heidelberg; 2009. p. 1131–7.
33. Atkins KM, Pashtan IM, Bussiere MR, Kang KH, Niemierko A, Daly JE, et al. Proton stereotactic radiosurgery for brain metastases: a single-institution analysis of 370 patients. Int J Radiat Oncol Biol Phys. 2018;101(4):820–9.
34. Particle Therapy Co-operative Group. Particle therapy facilities in clinical operation. 2018. Available from: https://www.ptcog.ch/index.php/facilities-in-operation.
35. Durante M, Loeffler JS. Charged particles in radiation oncology. Nat Rev Clin Oncol. 2010;7(1):37–43.
36. Schulz-Ertner D, Nikoghosyan A, Hof H, Didinger B, Combs SE, Jakel O, et al. Carbon ion radiotherapy of skull base chondrosarcomas. Int J Radiat Oncol Biol Phys. 2007;67(1):171–7.
37. Ares C, Hug EB, Lomax AJ, Bolsi A, Timmermann B, Rutz HP, et al. Effectiveness and safety of spot scanning proton radiation therapy for chordomas and chondrosarcomas of the skull base: first long-term report. Int J Radiat Oncol Biol Phys. 2009;75(4):1111–8.
38. Mizoe JE. Review of carbon ion radiotherapy for skull base tumors (especially chordomas). Rep Pract Oncol Radiother. 2016;21(4):356–60.
39. Kirkpatrick JP, Laack NN, Halasz LM, Minniti G, Chan MD. Proton therapy for brain metastases: a question of value. Int J Radiat Oncol Biol Phys. 2018;101(4):830–2.
40. Fossati P, Vavassori A, Deantonio L, Ferrara E, Krengli M, Orecchia R. Review of photon and proton radiotherapy for skull base tumours. Rep Pract Oncol Radiother. 2016;21(4):336–55.
41. Adeberg S, Harrabi S, Bougatf N, Verma V, Windisch P, Bernhardt D, et al. Dosimetric comparison of proton radiation therapy, volumetric modulated arc therapy, and three-dimensional conformal radiotherapy based on intracranial tumor location. Cancers. 2018;10(11):401.
42. Sperduto PW, Yang TJ, Beal K, Pan H, Brown PD, Bangdiwala A, et al. Estimating survival in patients with lung cancer and brain metastases: an update of the graded prognostic assessment for lung cancer using molecular markers (Lung-molGPA). JAMA Oncol. 2017;3(6):827–31.
43. Sperduto PW, Kased N, Roberge D, Xu Z, Shanley R, Luo X, et al. Effect of tumor subtype on survival and the graded prognostic assessment for patients with breast cancer and brain metastases. Int J Radiat Oncol Biol Phys. 2012;82(5):2111–7.
44. Ganong WF. Review of medical physiology. 21st ed. Boston: McGraw-Hill; 2003.
45. Yovino S, Kleinberg L, Grossman SA, Narayanan M, Ford E. The etiology of treatment-related lymphopenia in patients with malignant gliomas: modeling radiation dose to circulating lymphocytes explains clinical observations and suggests methods of modifying the impact of radiation on immune cells. Cancer Investig. 2013;31(2):140–4.
46. Petr J, Platzek I, Hofheinz F, Mutsaerts H, Asllani I, van Osch MJP, et al. Photon vs. proton radiochemotherapy: effects on brain tissue volume and perfusion. Radiother Oncol. 2018;128(1):121–7.
47. Huang J, DeWees TA, Badiyan SN, Speirs CK, Mullen DF, Fergus S, et al. Clinical and dosimetric predictors of acute severe lymphopenia during radiation therapy and concurrent temozolomide for high-grade glioma. Int J Radiat Oncol Biol Phys. 2015;92(5):1000–7.
48. Vaios EJ, Nahed BV, Muzikansky A, Fathi AT, Dietrich J. Bone marrow response as a potential biomarker of outcomes in glioblastoma patients. J Neurosurg. 2017;127(1):132–8.